The gas discharge visualization (GDV) order parameter model based on the principle of mastering both permanence and change

XIN Yu[a], ZHANG Lei[a], ZHAO Qiancheng[a], SHE Yurong[a, b], SHE Zhensu[a*], SONG Shuna[a*]

a. Institute of Health System Engineering and Department of Mechanics and Engineering Science, College of Engineering, Peking University, Beijing 100871, China

b. School of Traditional Chinese Medicine, Shandong University of Traditional Chinese Medicine, Jinan, Shandong 250355, China

ARTICLE INFO

ABSTRACT

Objective To investigate the human body's complex system, and classify and characterize the human body's health states with "a comprehensive integrated method from qualitative to quantitative".

Methods This paper introduces the concept of "order parameters" and proposes a method for establishing an order parameter model of gas discharge visualization (GDV) based on the principle of "mastering both permanence and change (MBPC)". The method involved the following three steps. First, average luminous intensity ($\bar{I}$) and average area ($\bar{s}$) of the GDV images were calculated to construct the phase space, and the score of the health questionnaire was calculated as the health deviation index (H). Second, the k-means++ clustering method was employed to identify subclasses with the same health characteristics based on the data samples, and to statistically determine the symptom-specific frequencies of the subclasses. Third, the distance (d) between each sample and the "ideal health state", which determined in the phase space of each subclass, was calculated as an order parameter describing the health imbalance, and a linear mapping was established between the d and the H. Further, the health implications of GDV signals were explored by analyzing subclass symptom profiles. We also compare the mean square error (MSE) with classification methods based on age, gender, and body mass index (BMI) indices to verify that the phase space possesses the ability to portray the health status of the human body.

Results This study preliminarily tested the reliability of the order parameter model on data samples provided by 20 participants. Based on the discovered linear law, the current model can use d calculated by measuring the GDV signal to predict H ($R^2 > 0.77$). Combined with the symptom profiles of the subclasses, we explain the classification basis of the phase space based on the pattern identification. Compared with common classification methods based on age, gender, BMI, etc., the MSE of phase space-based classification was reduced by an order of magnitude.

Conclusion In this study, the GDV order parameter model based on MBPC can identify subclasses and characterize individual health levels, and explore the TCM health meanings of the GDV signals by using subjective-objective methods, which holds significance for establishing mathematical models from TCM diagnosis principles to interpret human body signals.

*Corresponding author: SONG Shuna, E-mail: songshuna@pku.edu.cn. SHE Zhensu, E-mail: she@pku.edu.cn.

Citation: XIN Y, ZHANG L, ZHAO QC, et al. The gas discharge visualization (GDV) order parameter model based on the principle of mastering both permanence and change. Digital Chinese Medicine, 2024, 7(3): 231-240.

1 Introduction

Mastering both permanence and change (MBPC) is a fundamental principle in traditional Chinese medicine (TCM) diagnosis, encapsulating the concept of Yin-Yang balance [1]. MBPC aims to detect abnormal changes in excess or deficiency by recognizing the quasi-equilibrium state of the human body [1, 2], thus measuring deviations from an optimal health status. In this study, we aim to represent this diagnostic process mathematically: given the complexity of the system, it is essential to first categorize the objects involved and subsequently perform a local linearization of the quasi-equilibrium point within each subclass. This approach enables a quantitative assessment of how each object deviates from its respective quasi-equilibrium point.

From a fundamental perspective, human health represents a multi-scale equilibrium state characterized by complexity and dynamics. Western natural science approaches the human body through a mechanical view of life, employing reductionist method to study the human body's complex system. This leads to its research focus on fragmentary descriptions of phenomena of the human body, lacking a comprehensive theoretical model of the human body system [3]. Such limitations make it challenging to discern the holistic and nuanced patterns underlying these phenomena. This significantly limits the application of western scientific findings in personalized clinical diagnosis and treatment.

Therefore, it is crucial to identify parameters reflecting the circulation of Qi-blood from human signals, enabling the establishment of a model that describes both the balanced and deviant states of the human body system. MBPC offers a universal framework for interpreting physiological signals indicative of Qi-blood movement [4]. Currently, objective research on TCM diagnosis predominantly focuses on developing information-based tools that simulate the sensory skills of TCM practitioners — such as sight, touch, and smell — to align with four TCM diagnostic methods: inspection, auscultation and olfaction, inquiry, and palpation [5]. Advances in human signal measurement devices now allow for the sized collection of diverse physiological signals, underscoring the urgent need for a quantitative characterization of the Qi-blood movement patterns reflected by human body signals based on TCMD principles.

The gas discharge visualization (GDV) technique is an emerging quantum measurement technique that captures the human body's glow by acquiring Kirlian images of fingers, enabling quick and convenient assessment of health status [6, 7]. Widely applied in complementary and alternative medicine, traditional practices, psychophysiology, and consciousness research, the GDV technique aids in evaluating the effects of health management techniques [8]. Studies examining the correlations between GDV measurements and factors like heart rate variability, systolic and diastolic blood pressure, and stress level [9-11] suggest that GDV can measure autonomic nervous responses [12], making it valuable for assessing the impact of meditation on physical and mental health [13]. For instance, BHAT et al. [14] found a relationship between GDV image parameters and fasting blood glucose, which could support early diabetes diagnosis and treatment evaluation. Correlations between GDV image parameters and corresponding disease evaluation indicators have also been observed for conditions like hypertension and colon tumors [15-17]. Moreover, researchers have found that human body's glow changes dynamically with internal human body Qi-blood movement characteristics and its resonance with the external environment. For example, meditation, yoga, exercise, or different types of tea can all affect the human body glow [18-20]. This kind of research that explores the correlations between parameters and changes in human physiological state provides indicators that describe phenomena. However, these indicators lack clear physiological definitions in relation to the body's condition, making it challenging to elucidate the mechanism of Qi-blood movement underlying the correlations between indicators and phenomena.

Two main challenges arise in exploring the patterns of Qi-blood circulation in the human body as reflected in GDV signals. For one thing, the fluctuation range of GDV signal parameters is often larger than the variations induced by changes in health conditions. For another, relying on descriptive statistical approaches limits our understanding of human GDV signals, making it difficult to extract meaningful health-related information from the highly complex GDV signal system.

We propose that GDV technology should transition from observational research to establishing interpretable mathematical modeling research. Given the numerous factors influencing health and the considerable variability among individuals, it is essential to adopt a comprehensive integrated approach from qualitative to quantitative in human studies. Professor SHE Zhensu, building on QIAN Xuesen's concepts in human science, proposed a human body model of "one element, two sides, multi-dimensional and multi-level" [21]. This model underscores the presence of multi-dimensional and multi-level Yin-Yang balances and self-organization centers in the human body system. We hold the belief that any signal capable of reflecting alterations in Qi-blood and Yin-Yang dynamics can be extracted from the principles of TCM diagnosis, rooted in Yin-Yang balance. By extracting appropriate parameters, we can establish mathematical models that define a quasi-equilibrium state and interpret physiological meaning based on the physical principles underlying the measurement signals.

This study aims to extract parameters from GDV signals that reflect variations in Qi-blood. Grounded in the

MBPC TCM framework, it seeks to develop a mathematical model for classifying and quantifying complex health quasi-equilibrium states. Furthermore, the physiological significance of the measured signals will be elucidated based on their underlying physical principles.

2 Data and methods

This paper presents a method that combines subjective and objective measurements, drawing on the "order parameter" model. The theory of human body order parameters is applied to classify and quantify complex quasi-equilibrium health states [22, 23], providing a mathematical expression of the basic principle of MBPC. This method preliminarily constructs a quantitative relationship between GDV image signal parameters and the health deviation index, aiming to describe the health quasi-equilibrium state and its deviations.

Specifically, the method proceeds in three steps. First, we determined the key parameters of the GDV image's average luminous intensity ($\bar{I}$) and average area ($\bar{S}$) to reflect the Qi-blood and Yin-Yang dynamics by analyzing the correlation between GDV image parameters and health questionnaire results. Phase space is constructed to distribute sample data points. Second, we automatically clustered data samples within phase space. According to the elbow method of fitting degree (R^2), we identified three clusters, representing three different types of health status, termed as "subclasses". Finally, according to health questionnaire results, each subclass is associated with an ideal health state, characterized by high order and minimal questionnaire symptoms. From this, we measured the deviation degree (d) between each sample and the ideal health state. A greater d indicates a lower system orderliness of the human body. Showing a linear relationship between them, d is termed as the order parameter. Based on a linear relationship between d and the health deviation index (H), we described human health status by measuring the GDV signal.

2.1 Participants

In this study, under informed consent, participants without clinical diseases diagnosed by western medicine were recruited from the Peking University campus and community. Data collection took place from March 1 to June 20, 2021. The inclusion and exclusion criteria are as follows.

2.1.1 Inclusion criteria (i) Age between 17 and 90 years, any gender. (ii) Absence of significant somatic diseases, abnormal indicators, and history of mental disorders. (iii) Signed informed consent form.

2.1.2 Exclusion criteria (i) Individuals with cardiac pacemakers. (ii) Individuals with artificial implants, such as neurostimulators, insulin pumps, electronic cochlear implants, or other implanted charged devices. (iii) Individuals unable to maintain physical stability during measurement due to mental or physical reasons. (iv) Individuals with a history of acute diseases or trauma within two weeks prior to the experiment.

2.2 GDV measurement

Using the GDV measuring equipment at the ENN Institute of Life Science and Technology, we acquired ten-finger signals based on the following principles [8]. When an object is placed in an electromagnetic field and subjected to a strong electric pulse, it emits excited photons and electrons, a process termed "photon-electron radiation". The light produced is recorded by a camera with a sensitive charge-coupled device (CCD), which converts the radiation into a color computer image or bio-image. This process represents the basic physical principle of GDV imaging (Figure 1).
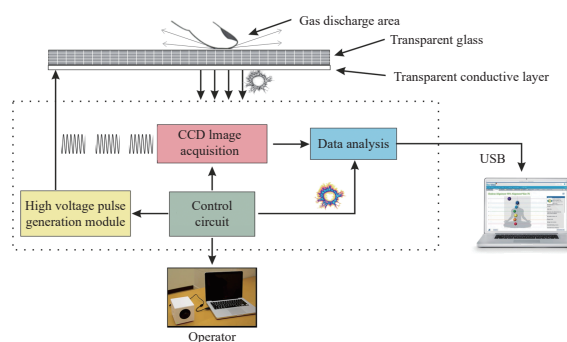
Figure 1 GDV hardware principle function block diagram [24]

It is important to note that if the subject accidentally touches the grounded metal or conductive surfaces during GDV measurement, they may experience a strong electric shock sensation. To ensure accuracy, the finger and the screen should be cleaned before each measurement to prevent contaminating the screen from impurities and affecting the measurement results. Additionally, maintaining a consistent hand position across multiple measurements is recommended to improve reliability.

2.3 Health questionnaire

The health questionnaire used in this study is based on TCM diagnosis syndrome element theory [25]. It is designed to gather information on common symptoms of non-health manifestations of the human body and measure the health level of participants. The questionnaire includes 105 questions, each rated on a 5-point scale: 0 represents "rarely", 1 "occasionally", 2 "sometimes", 3 "often", and 4 "almost always". Participants were asked to answer each question according to their real feelings in recent months. Scores were then totaled to calculate each

participant's H

$$H = \frac{\sum_1^N x_i}{S} \tag{1}$$

Where x_i is the actual score of each question, N is the number of questions in the questionnaire, and S is the full score of the questionnaire. Here, $N = 105$, $S = 420$.

From the perspective of the MBPC principle, all symptoms are manifestations of a deviation from the quasi-equilibrium state [26]. In an ideal health state, the human body reaches the highest system orderliness, showing no symptoms on a macroscopic level, with $H = 0$. When there is a deviation from this ideal state, the system orderliness of the human body decreases. It shows symptoms macroscopically, $H \neq 0$. According to Equation (1), the value range of the H is $[0, 1]$. It is an order parameter reflecting the system orderliness of the human health state.

2.4 Building GDV order parameter model

Drawing on Landau's concept of the order parameter, this paper proposes a GDV order parameter model. The order parameter serves as a measure of the system orderliness. Given the multi-dimensional and multi-level complexity of the human body, it is difficult to describe its health state with simple linear laws. However, by dividing it into multiple subclasses, we can uncover linear patterns by refining order parameters within each subclass. The core value of the order parameter, therefore, lies in enabling quantitative processing within a qualitative classification framework. In this study, we used the health deviation index as an order parameter to measure the system orderliness of health state. When a GDV parameter is found to exhibit a simple linear relationship with this index, this parameter can likely be identified as an order parameter.

We defined characteristic distance in two-dimensional phase space composed of key health parameters (average luminous intensity ($\bar{I}$) and average area ($\bar{S}$), see Supplementary material for parameter definition)

$$d = \sqrt{\left(\bar{S}_i - \bar{S}_{\text{best}}\right)^2 + \left(\bar{I}_i - \bar{I}_{\text{best}}\right)^2} \tag{2}$$

Where ($\bar{S}_{\text{best}}, \bar{I}_{\text{best}}$) is the position of the "ideal health state" of this subclass in phase space. Assume that there is a linear relationship between deviation degree d and health deviation index H, which is

$$H = k * d + b \tag{3}$$

When $\bar{S}_i = \bar{S}_{\text{best}}$, $\bar{I}_i = \bar{I}_{\text{best}}$, there is

$$b = H_{\text{best}} \tag{4}$$

That is, b is the best health deviation index corresponding to the ideal health center. Substitute Equation (4) into Equation (3) to get

$$k = \frac{H_i - H_{\text{best}}}{d} = \frac{\Delta H_i}{d} \tag{5}$$

Where ΔH_i is the change value of the health deviation index relative to the best health deviation index. d represents the deviation of the sample point from the ideal health center. The ratio demonstrates the sensitivity of health state changes to variations in characteristic distance within this subclass. A smaller $|k|$ indicates a less sensitive response of the health state to deviations in GDV degree, whereas a larger $|k|$ implies a higher level of sensitivity.

We used Pytorch to establish a linear model and determine the ideal health center ($\bar{S}_{\text{best}}, \bar{I}_{\text{best}}$) and model parameters k and H_{max}. After defining model parameters, we choose mean square error (MSE) as the loss function, and make mean square error between model predicted health deviation index $f(d_i)$ and actual measured health deviation index H_i minimum

$$\left(\bar{S}_{\text{best}}, \bar{I}_{\text{best}}, k, H_{\text{max}}\right) = \arg\min \sum_{i=1}^m \left(f(d_i) - H_i\right)^2 \tag{6}$$

Where m is the number of samples in this subclass.

2.5 Determining subclasses with the same health characteristics

It is evident that data exhibit convexity in the phase space, following the principle of MBPC. In the phase space constructed by key health parameters (average luminous intensity ($\bar{I}$) and average area ($\bar{S}$), we employed the classic k-means++ method to cluster the data with normalization performed before clustering. Using the elbow method based on fitting degree (R^2), we classified all data accordingly.

2.6 Analysis the symptom spectrum of subclasses

To investigate the health characteristics of distinct subclasses, we conducted a statistical analysis of the symptom frequency from the health questionnaire. By calculating the specific symptoms (according to the normalised frequency of occurrence of a symptom in the samples in the subclass, greater than 0.8 being a high frequency symptom, less than 0.5 being a low-frequency symptom) that emerged within each subclass, we were able to delineate and discuss the underlying characteristics of Qi-blood movement. This analysis was grounded in the physical meaning of the two GDV parameters.

2.7 Comparison with traditional classification methods

We contend that the classification of the order parameter model, grounded in the phase space analysis, captures the core commonality of the population. Consequently, when employing this model to forecast health deviation

degrees, it exhibits superior cohesion within subclasses, outperforming other conventional classification methods such as gender, age, and body mass index (BMI). This advantage can be quantitatively reflected through specific error indicators. In this study, we selected two error indicators: MSE and mean relative error (MRE) (see Supplementary material). We calculated the model fitting error for each subclass.

$$MSE = \frac{1}{m} \sum_{i=1}^{m} \left(H_i - \hat{H}_i \right)^2 \tag{7}$$

This error indicator is a more convenient means to quantify the "average error", which is the difference between the health index estimate and the true value. A smaller MSE value indicates that the prediction model more accurately describes the experimental data. Similarly,

$$MRE = \frac{100\%}{m} \sum_{i=1}^{m} \frac{\left| H_i - \hat{H}_i \right|}{\bar{H}} \tag{8}$$

is the ratio of the absolute error between the health index estimate and true value, and the average value of multiple measurements. It provides a clearer perspective on the order of magnitude difference of absolute errors between model estimates and true values.

To validate this hypothesis, we classified data according to gender, age, BMI, and three common human physiological characteristics, respectively. We then compared fitting results under different classification conditions.

3 Results

3.1 Data collection

We collected data from 20 volunteers to build the model. All participants' ten-finger GDV images and health questionnaire responses were collected. The distribution of their gender, BMI, and age are shown in Table 1. To reduce measurement error, each participant completed three consecutive measurements. GDV parameters were calculated for results of three measurements respectively for the same measurer, and the averages were taken as final GDV signal parameters for the measurer.

Table 1 Physiological characteristics of data samples

Characteristic	Category	Sample size
Gender	Male	8
	Female	12
BMI	< 18.5	5
	18.5 – 24	8
	> 24	7
Age	18 – 20	6
	20 – 24	9
	> 24	5

3.2 General linear law of subclass division based on phase space

Typical GDV measurement images for each subclass are shown in Figure 2A – 2C. We designated blue dots as full class (n = 5), red dots as moderate class (n = 8), and brown dots as lacking class (n = 7) based on the visual characteristics of the subclasses.

Moreover, we observed a strong linear relationship between d and H after determining the ideal health center of three subclasses. Figure 2D – 2F show that the health deviation index rises with the increase of d for three subclasses. Table 2 presents the fitting results of the
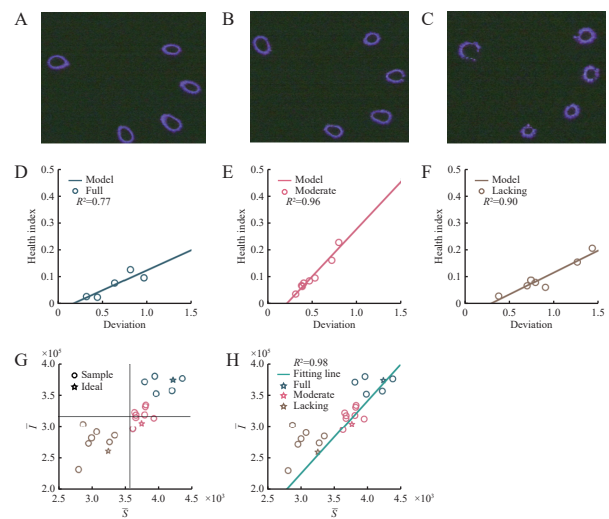
Figure 2 Subclass division and model parameter optimization of data samples in phase space

A – C, typical GDV measurement images (left hand) representing three subclasses, corresponding to bright and full type, moderate type, and dark and sparse type, respectively. The circles in the figure represent actual data samples, and the straight line represents the fitting result of the model. D – F, fitting results of full class (n = 5), moderate class (n = 8), and lacking class (n = 7) models, respectively. G, the distribution of subclasses in $\bar{S}$ – $\bar{I}$ phase space and the position of ideal points, where the black solid line indicates the parameter average value of all samples. Analyzing the parameter characteristics of distribution, blue dots correspond to the subclass with the largest $\bar{S}$ and $\bar{I}$, manifesting as bright and full halos in the GDV images; brown dots represent the subclass with smaller $\bar{S}$ and $\bar{I}$, reflected as dark and missing halos in the GDV images; while red dots, falling between the two, are reflected in the GDV images as intermediate in brightness and fullness. H, the distribution position of ideal points in phase space having a linear relationship. The circles in the figure represent the actual data samples, and the pentagrams are the ideal health centers given by the model.

Table 2 Model fitting parameter results obtained from GDV order parameter space classification

Subclass	Size	k	b	R^2
Full class	5	0.15	– 0.027	0.77
Moderate class	8	0.36	– 0.077	0.96
Lacking class	7	0.17	– 0.050	0.90

model, with an R^2 value of 0.77 for the full class and both other subclasses having R^2 values greater than 0.9.

Significantly, Figure 2G illustrates the distribution of 20 samples in phase space, which constructed from two key parameters extracted from $\bar{S}$ and $\bar{I}$. Utilizing the common elbow method, the dataset of 20 samples was optimally clustered into three subclasses, corresponds exactly to the apparent visual differences observed in the typical GDV images of the subclasses. Figure 2H depicts a reliable linear relationship between ideal health points of three subclasses ($R^2 = 0.98$).

These findings provide robust evidence that there is a general linear law between health status and d within a subclass, and d serves as a key order parameter revealing this evolution law.

3.3 Explaining the physiological meaning of GDV signal through subclass symptom spectrum

We observed that the distributions of the symptom spectra of different subclasses exhibit distinct differences. Figure 3 shows the distribution of the symptom spectrum of each category, clearly highlighting that the high-frequency ($F > 0.8$) symptoms of the full class are mainly "spontaneous sweating".

The horizontal axis represents the specific symptom spectrum that distinguishes the three subclasses. The vertical axis denotes different subclasses. The numbers in the grid mark the frequency of a certain symptom in a certain subclass; darker shades signify higher frequencies. The symptom spectrum includes all symptoms that have a frequency higher than 0.7 in at least one class and a standard deviation greater than 0.15 among the three classes. The symptoms are sorted from left to right according to the frequency of the lacking class.

Table 3 demonstrates the different specific symptoms of subclasses. For the moderate class, the high-frequency symptoms are "vexation" and "decreased attention span", whereas the lacking class exhibits high-frequency symptoms such as "fear and anxiety" and "insomnia and excessive dreaming". Each subclass had specific high-frequency symptoms and was highly differentiated.
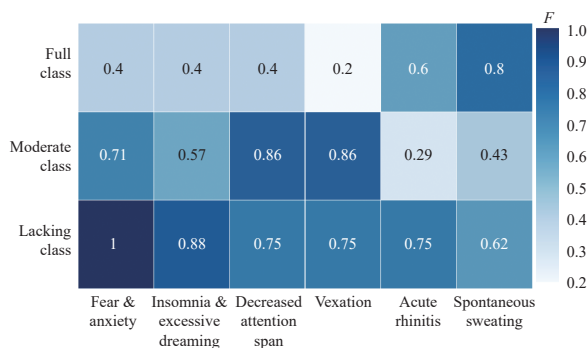
Figure 3 Symptom spectrum distribution of each subclass

Table 3 Mean health deviation index and specific symptoms for each subclass

Subclass	$\bar{H}$	Specific symptom	
		High-frequency ($F > 0.8$)	Low-frequency ($F < 0.5$)
Full class	0.068	Spontaneous sweating	Fear and anxiety insomnia excessive dreaming vexation decreased attention span
Moderate class	0.101	Vexation decreased attention span	Spontaneous sweating acute rhinitis
Lacking class	0.097	Fear and anxiety insomnia excessive dreaming	–*

–* means there were no such symptoms.

3.4 Comparison of phase space order parameter model with general classification methods

The artificial subclass division according to different human physiological characteristics and the fitting results of the model are presented in Table 4. Apart from gender, age and BMI were both categorized into three classes, ensuring a comparable number of samples in each subclass.

Table 4 Classification according to gender, age, and BMI and model fitting parameter results obtained

Characteristic	Category	Size	R^2	MSE	MRE
Gender	Female	12	0.14	395.96	0.049
	Male	8	0.00	126.80	0.031
Age	18 – 20	6	0.00	216.51	0.048
	20 – 24	9	0.52	72.74	0.020
	> 24	5	0.00	238.71	0.060
BMI	< 18.5	5	0.35	123.48	0.052
	18.5 – 24	8	0.82	17.34	0.013
	> 24	7	0.00	330.19	0.066

The model fitting error obtained by the phase space classification method was lower than that obtained by using common human physiological characteristics to classify the population. Figure 4A presents comparison of MSE of model fitting under four classification methods. The fitting result MSE using phase space for classification was only 17.8, which is much lower than other classification methods. The result indicates that, in contrast to using traditional human characteristics (BMI, gender, and age) for population classification, classifying the population through order parameter phase space captures the core health state system orderliness of the subclass population.

To ascertain whether varying the number of classifications impacts the accuracy of the model, we varied the number of subclasses for testing. Figure 4B illustrates the trend of MSE of model fitting results as the cluster

number k is adjusted within the range of 1 to 5 under three classification methods: phase space, age, and BMI. Across various classification numbers, the fitting error of the phase space classification method remained significantly lower than that of age and BMI in these two classification methods. Additionally, we observed that increasing the number of classified data did not lead to a better-fitting result for the model. We noted that as the number of classes increased from 3 to 4, the average relative error increased. This finding underscores the inherent structural characteristics within the data, which serve as the basis for the qualitative division of health state subclasses.
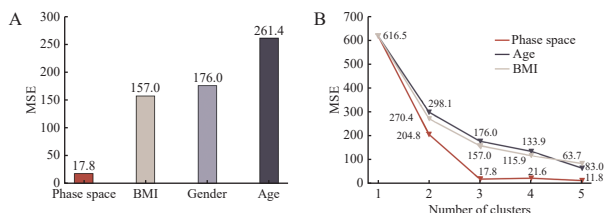
Figure 4 Fitting error of model under different classification methods and numbers of classes
A, the fitting error of the model under various classification methods and the number of classes. B, the influence of different cluster numbers on the fitting error of the model. Different colors are employed to distinguish between the classification indicators (red represents phase space, dark gray indicates age, and beige signifies BMI).

4 Discussion

4.1 The significance of phase space diagram for molecular classes

Ideal health points of three subclasses were linearly distributed in phase space, suggesting the potential of phase space to describe the evolution of different population health patterns. The phase space is an ordered space depicting the evolution among different subclasses, providing a basis for our inference that the health mode alterations of each subclass follow a regular pattern. From this inference, a more valuable thing is that constructing phase space can divide the population into subclasses based on the first principle, offering significant support for artificial intelligence-assisted medical treatment. In our research, we also found that when the cluster number was set as $K = 4$, the sample point in the lower left corner of the dark missing subclass was separated into one class alone. Consequently, this observation leads us to speculate that another subclass exists in the lower left corner of the phase space (Figure 2). This hypothetical subclass is characterized by a very dark halo with many gaps. This requires further verification through the collection of additional data.

In contrast to traditional machine learning approaches that rely on labeled data, the physical meaning of the GDV signal corresponding to subclass division in phase

space is clear, facilitating iterative engagement with clinical experiments and a deeper understanding of the health implications reflected by signal. The linear law expression varies within different subclasses, indicating that each subclass corresponds to several stable states commonly experienced by individuals, aligning with the idea of the TCM diagnosis principle. This will be explored in greater depth in section 4.2.

4.2 Physiological characteristics of GDV physical parameters

Among the three subclasses, the average value of the health deviation index increases in sequence. We can preliminarily conclude that the "full class" represents the optimal health state. Combining the physical principle of GDV imaging (as outlined in the method section) and the principle of Yin-Yang balance in TCM diagnosis, we offer the following interpretation of the physiological characteristics associated with GDV parameter variations.

Conjecture from the perspective of physics, when the overall system orderliness of the human body is high, the overall conductivity is also high, resulting in strong photoelectric radiation at the fingertip; conversely, when the system orderliness of the human body decreases, the overall conductivity lowers, leading to weaker photoelectric radiation at the fingertip.

Therefore, we can surmise that the halo image's $\bar{S}$ represents the contact angle and area between fingertip tissue and the halo panel, which indicates the Qi-blood filling degree on the human body surface. Under constant voltage, the distance from fingertip discharge to break through the air to reach conductive film is determined, while a person in optimal health should exhibit well-developed and resilient fingertip tissue and $\bar{S}$ of its halo image should be within a moderate range. If $\bar{S}$ is too small, it suggests that fingertip tissue is too dry and lacks elasticity or is too tight. From the perspective of TCM diagnosis theory, it corresponds to the human body Qi being too inwardly convergent, indicating a Yang-deficient type. If $\bar{S}$ is too large, it indicates that fingertip tissue is too loose and lacks wrapping force. It corresponds to the human body Qi being too outwardly divergent, characteristic of a Yin-deficient type.

Under the same condition of $\bar{S}$, average brightness $\bar{I}$ of the halo is related to human body conductivity, which in turn depends on the smoothness of Qi-blood. A person in better health should exhibit stable and moderate skin electricity at the fingertip. The average brightness $\bar{I}$ of its halo should be within a moderate range. If the average brightness $\bar{I}$ is too small, it indicates that the skin's electric property at the fingertip is not very active. It corresponds to the inactive operation of Qi on the body surface. From the perspective of TCM diagnosis theory, it may be caused by Qi-blood movement obstruction

brought by excess pathogenic Qi or insufficient vital Qi leading to inwardly convergent Qi. If the average brightness $\bar{I}$ is too high, it suggests that the skin's electric property at the fingertip is excessively active. It corresponds to the significant operation of Qi on the body surface, which may be due to excessive Yang Qi causing outwardly divergent Qi.

From these insights, we can qualitatively determine the changing patterns of Qi-blood and Yin-Yang in the human body through the changes in the key parameters of GDV, thus explaining the differences between the symptom profiles of the three subclasses. For example, according to TCM evidence theory, the evidence type of "full class" is inclined towards the "the exterior is not consolidated" pattern, indicative of insufficient energy astringency. Conversely, the evidence type of "lacking class" is more aligned with the "phlegm obstructing the heart vessels pattern", reflecting an internal blockage, where the meridians do not flow smoothly.

Considering the consensus on the human health implications of the classification results obtained from TCM theory and phase space, the difference in symptom spectrum reflects the phenomenon that samples within the same subclass share similar human body function characteristics, whereas the differences of samples across different classes are substantial. This suggests that our approach of using an order parameter model to construct a phase space and then classifying the population in the phase space is advantageous for describing the self-organization of complex systems in the human body.

It suggests that our approach of using an order parameter model to construct a phase space and then classifying the population in the phase space is advantageous for describing the self-organization of complex systems in the human body. The method is characterized by the use of an order parameter model to determine the ideal health points in the subclasses and to calculate the deviation of the sample points relative to the ideal health points, thereby quantitatively describing the changes in health states and thus mathematically expressing the TCM diagnosis principle. In future work, we intend to collect more data and carry out more detailed correlation research on a larger scale.

4.3 Advantages of phase space order parameter model compared with general classification methods

Figure 4 reveals that data with common health states in GDV parameter phase space exhibit clustering, indicating that clustering methods can be employed to differentiate between these subclasses. Under different health types, the evolution law of the health states adheres to a consistent linear law as characterized by the deviation degree, which is represented by the GDV deviation degree d. This d serves as an order parameter that quantifies the system orderliness of health states within subclasses. The model based on the health deviation degree is found to be more accurate than classification results derived from human physiological characteristics such as age, gender, and BMI.

However, compared with the accuracy and universality of the proposed model, the greater significance of this study lies in the mathematical resolution we propose for the TCM diagnosis and treatment idea of "treatment based on pattern differentiation". This approach holds two significant advantages for clinical application. First, the scheme provides a modeling method for TCM practitioners to combine subjective and objective information in the process of "treatment based on pattern differentiation". This method takes into account the correlation between physical principles, objective parameters, TCM theories, subjective feelings, and other information, thereby facilitating patient health status recognition and enhancing patient compliance. Second, the scheme provides a diagnostic reference and basis for TCM practitioners, particularly for complex diseases and patients requiring long-term treatment who may be challenging to diagnose accurately at the outset. The program enables TCM practitioners to make tailored diagnoses and treatment plans by subcategorizing and identifying similar cases within subcategories, even when encountering novel health states. This empowers practitioners to adapt their diagnosis and treatment strategies according to the model.

4.4 Limitations and prospects

This study does have some limitations. First, the sample size of this study is relatively small and participants in this study are primarily college students with similar health statuses, which makes it challenging to discern the system orderliness of health states within subclasses. Second, the significant changes in system orderliness within subclasses underscore the need for cross-validation techniques and additional external validation to ensure the model's generalizability when applied to a larger, independent dataset. Finally, although the present study attempts to correlate GDV parameters with health status by aligning with TCM theory, the underlying biomolecular dynamics mechanisms behind these correlations are not fully elucidated and warrant further investigation using a more comprehensive set of measures. Future studies will include a larger and more diverse sample to validate the model's robustness. We aspire to collaborate with hospitals to conduct long-term observations of patients with chronic diseases such as hypertension to incorporate more cases as well as longitudinal data. This approach will not only enhance our in-depth understanding of the changes in health status over time but also optimize the proposed model and delve deeper into the biological mechanisms and physical basis of GDV parameters.

5 Conclusion

We propose a mathematical model for analyzing health states, grounded in the TCM diagnosis principle and the physical principles of GDV measurement. This model presents a mathematical interpretation for the diagnosis pattern of TCM syndrome differentiation and treatment. In clinical practice, Chinese medicine practitioners categorize patients into different syndrome types based on symptoms and assess the severity of each syndrome type. We have developed a GDV serial parameter model to mathematically represent this process.

This study holds significant implications for health state analysis based on GDV signals. Analysis of the symptom profiles of the subclasses revealed that GDV signals contain highly structured features reflecting the fluctuations of Qi-blood in the human body, which can guide the development of visualization techniques for timely and personalized clinical observation of the Yin-Yang balance.

This study provides insights into the feasibility of utilizing order parameter method to mathematize the TCM diagnosis process, under the guidance of complex system research methodology. By linking the physical principles of GDV signals to the fluctuations of Qi-blood in the human body, according to the Yin-Yang balance theory, we have elucidated the mechanism behind changes in human health states. We have grounds to believe that the physiological signals obtained by any instrument or equipment (such as GDV) capable of measuring the fluctuations of Qi-blood in the human body can manifest the TCM diagnosis principle of the Yin-Yang balance.

Competing interests

The authors declare no conflict of interest.

References

[1] LI MZ, CAI YY, WANG YP, et al. The principle of "constant variation" diagnosis and its application in traditional Chinese medicine. China Journal of Traditional Chinese Medicine and Pharmacy, 2022, 37(9): 5152–5154.

[2] WANG ZX. The enlightenment of TCM diagnosis and treatment thinking to narrative nursing. Chinese Journal of Intergrative Nursing, 2022(11): 2, 5.

[3] SONG SN, SHE ZS. Quantum theory-based physical model of the human body in TCM. Digital Chinese Medicine, 2022, 5(4): 354–359.

[4] STEVENSON X, TAI S, YUAN C. Handbook of Traditional Chinese Medicine (In 3 Volumes). Singapore: World scientific, 2014.

[5] ZHANG Q, ZHOU JH, ZHANG B. Computational Traditional Chinese Medicine diagnosis: a literature survey. Computers in Biology and Medicine, 2021, 133: 104358.

[6] KOROTKOV K. Review of EPI papers on medicine and psychophysiology published in 2008-2018. International Journal of Complementary & Alternative Medicine, 2018, 11(5): 311–315.

[7] KOSTYUK N, COLE P, MEGHANATHAN N, et al. Gas discharge visualization: an imaging and modeling tool for medical biometrics. International Journal of Biomedical Imaging, 2011, 2011: 196460.

[8] BISTA S, JASTI N, BHARGAV H, et al. Applications of gas discharge visualization imaging in health and disease: a systematic review. Alternative Therapies in Health and Medicine, 2023, 29(6): AT6764.

[9] CIOCA G, GIACOMONI P, REIN G. A correlation between GDV and heart rate variability measures: a new measure of well being. Geneva: Backbone Publishing, 2004: 59–65.

[10] ALEKSANDROVA EV, ZARUBINA TV, KOVELKOVA MN, et al. GDV analysis of arterial hypertension. Seattle: Amazon Publishing, 2011: 191-201.

[11] KOROTKOV K. Energy fields electrophotonic analysis in humans and nature. Sudbury: eBookIt. Com, 2013.

[12] KOROTKOV KG. Gender differences in the activity of the autonomic nervous systems of healthy and hypertensive patients in Russia. Journal of Applied Biotechnology & Bioengineering, 2017, 3(6): 00084.

[13] KUSHWAH KK, SRINIVASAN TM, NAGENDRA HR, et al. Effect of yoga based techniques on stress and health indices using electro photonic imaging technique in managers. Journal of Ayurveda and Integrative Medicine, 2016, 7(2): 119–123.

[14] BHAT RK, MAVATHUR R, SRINIVASAN TM. Diabetes mellitus type 2 and Yoga: electro photonic imaging perspective. International Journal of Yoga, 2017, 10(3): 152–159.

[15] YAKOVLEVA EG, BUNTSEVA OA, BELONOSOV SS, et al. Identifying patients with colon neoplasias with gas discharge visualization technique. Journal of Alternative and Complementary Medicine, 2015, 21(11): 720–724.

[16] KOROBKA IE, YAKOVLEVA EG, KOROTKOV KG, et al. Electrophotonic imaging technology in the diagnosis of autonomic nervous system in patients with arterial hypertension. Journal of Applied Biotechnology & Bioengineering, 2018, 5(1): 112–116.

[17] NARANJAN R. EPI readings of type II diabetes. Proceedings of International Scientific Congress on Bioelectrography, 2018: 16-23.

[18] KUMAR KS, SRINIVASAN TM, ILAVARASU J, et al. Classification of electrophotonic images of yogic practice of mudra through neural networks. International Journal of Yoga, 2018,

11(2): 152–156.

[19] DROZDOVSKI A, GROMOVA I, KOROTKOV K, et al. Express-evaluation of the psycho-physiological condition of Para-lympic athletes. Open Access Journal of Sports Medicine, 2012, 3: 215–222.

[20] JIN WL, TAO YC, WANG C, et al. Infrared imageries of human body activated by tea match the hypothesis of meridian system. Phenomics, 2023, 3(5): 502–518.

[21] SHE Z, NI Z. Scientific exploration of human complexity system. Beijing: China Science Publishing & Media, 2012.

[22] ZHANG L. Study on human order parameters applied to COVID-19 evolution and pulse wave analysis. Beijing: Peking University, 2022.

[23] ZHANG L, SHE YR, SHE GH, et al. The cross-scale correlations between individuals and nations in COVID-19 mortality. Scientific Reports, 2022, 12(1): 13895.

[24] KOROTKOV K. Diagnosis and monitoring of the human energy-informational state and analysis of subtle energies, applying Gas Discharge Visualization technique, based on the Kirlian method. Saint Petersburg: Peter the Great St.Petersburg Polytechnic University, 2007.

[25] ZHU WF, YAN JF. 2005. The content and scientific significance of a new syndrome differentiating system based on new pattern element. Medicine & Philosophy, 26(1): 69–70.

[26] ZHANG B, WU M. Internal Medicine of TCM. Beijing: China Press of Traditional Chinese Medicine, 2017.

基于知常达变原理的气体放电可视化（GDV）序参量模型

忻煜[a], 张磊[a], 赵前程[a], 佘钰嵘[a,b], 佘振苏[a*], 宋舒娜[a*]

a. 北京大学工学院健康系统工程研究所, 北京 100871, 中国
b. 山东中医药大学中医学院, 山东 济南 250355, 中国

【摘要】目的 采用"从定性到定量的综合集成法"来研究人体复杂系统，以实现对人体健康状态的定性分类和定量刻画。方法 本文通过引入"序参量"的概念，提出了基于"知常达变"原理建立气体放电可视化（GDV）图像信号的序参量模型的方法，分为三个步骤。首先，计算 GDV 图像的平均亮度（$\bar{I}$）和平均面积（$\bar{S}$）构建相空间，并计算健康问卷的总得分作为健康偏差指数（H）；其次，采用 k-means++ 聚类方法，根据数据样本确定具有相同健康特征的亚类，统计各个亚类的特异性症状频次。最后，在相空间中确定每个亚类的"理想健康状态"，计算每个样本与其之间的距离（d）作为描述健康偏离度的序参量，建立 d 与 H 之间的线性映射。进一步的，通过分析亚类症状谱，探索 GDV 信号的健康含义。我们还与基于年龄、性别和体质指数（BMI）的分类方法比较均方误差（MSE），来验证相空间具备刻画人体健康状态的能力。结果 本研究初步在 20 名志愿者提供的数据样本中检验了序参量模型。基于发现的线性规律，当前模型可以通过 GDV 图像信号计算得到的偏差（d）来预测健康偏差指数（H）（$R^2 > 0.77$）。结合亚类的症状谱，我们为相空间的分类依据提供了基于辨证论治的解释。与基于年龄、性别、BMI 等的常见分类方法相比，基于相空间分类的 MSE 降低了一个数量级。结论 本研究基于"知常达变"原理的 GDV 图像信号序参量模型能够准确地识别亚类并表征个体的健康水平，采用主客观结合的方法探索 GDV 信号的中医健康含义，对于从传统中医诊断原理建立数学模型以解读人体信号具有重要意义。

【关键词】气体放电可视化；中医；序参量；数理模型；个性化健康评估